*China Ocean Eng.*, 2017, Vol. 31, No. 4, P. 458–465
DOI: 10.1007/s13344-017-0043-0, ISSN 0890-5487
http://www.chinaoceanengin.cn/ E-mail: coe@nhri.cn

# Wave Power Focusing due to the Bragg Resonance

TAO Ai-feng[a, b], YAN Jin[b], WANG Yi[b], ZHENG Jin-hai[a, b, *], FAN Jun[b], QIN Chuan[c]

[a]State Key Laboratory of Hydrology-Water Resources and Hydraulic Engineering, Hohai University, Nanjing 210098, China

[b]College of Harbor Coastal and Offshore Engineering, Hohai University, Nanjing 210098, China

[c]College of Energy and Electrical Engineering, Hohai University, Nanjing 210098, China

Received September 22, 2016; revised March 23, 2017; accepted May 22, 2017



**Abstract**

Wave energy has drawn much attention as an achievable way to exploit the renewable energy. At present, in order to enhance the wave energy extraction, most efforts have been concentrated on optimizing the wave energy convertor and the power take-off system mechanically and electrically. However, focusing the wave power in specific wave field could also be an alternative to improve the wave energy extraction. In this experimental study, the Bragg resonance effect is applied to focus the wave energy. Because the Bragg resonance effect of the rippled bottom largely amplifies the wave reflection, leading to a significant increase of wave focusing. Achieved with an energy conversion system consisting of a point absorber and a permanent magnet single phase linear motor, the wave energy extracted in the wave flume with and without Bragg resonance effect was measured and compared quantitatively in experiment. It shows that energy extraction by a point absorber from a standing wave field resulted from Bragg resonance effect can be remarkably increased compared with that from a propagating wave field (without Bragg resonance effect).

**Key words:** wave power, experiment, Bragg resonance

**Citation:** Tao, A. F., Yan, J., Wang, Y., Zheng, J. H., Fan, J., Qin, C., 2017. Wave power focusing due to the Bragg resonance. China Ocean Eng., 31(4): 458–465, doi: 10.1007/s13344-017-0043-0

## 1 Introduction

Wave power development has drawn much attention due to its immense energy potential along the coastlines worldwide, especially in the sea area that prevails westerly winds between 30°–60° latitude in northern and southern hemisphere (Falcão, 2010). In Chinese coastal line, the estimated total wave energy is about 12.8 GW, but the wave energy power density around coastal area is only 3–7 kW/m, which belongs to low wave energy density (Shi et al., 2011).

In order to extract the wave energy, usually there are three stages for wave energy conversion (Zhang et al., 2013). The first stage is the wave body, which gathers the wave energy and keeps the motion of itself. The second stage is an intermediate conversion device. This stage aims to convert the wave's kinematic energy absorbed by the wave body into the available mechanical energy. The third stage is the power generation equipment, in which the mechanical energy is converted to electrical energy through the generator.

Although noticeable progresses of the wave energy extraction have been made in the past few decades along with broad application prospects, wave energy capture and extraction still encounter many problems especially the relatively low conversion rate. So many efforts have been devoted to the technologies to improve the conversion efficiency in mechanical and electrical ways. Various specific mechanical devices have been designed and applied into preliminary test.

However, enhancing the wave energy density in the sea area for wave power exploitation was ignored, because the wave height in sea areas is thought to be naturally determined in conventional thinking. So, all the attentions were paid to find the sea areas with high wave energy density and to improve the wave energy equipment's conversion rate. But the sea areas with high wave energy density are mostly far away from the coastal line, and it will cost much to lay the power transmission cable system. Paradoxically, in shallow water coastal regions near the coastal line, the wave en-

Foundation item: This research work was financially supported by the National Natural Science Fundation of China (Grant Nos. 51579091, 51379071, and 51137002), the Qing Lan Project of Jiangsu Province, the Basic Research Fund from the State Key Laboratory of Hydrology-Water Resources and Hydraulic Engineering, Hohai University (Grant Nos. 20145027512 and 20145028412), the Short-term Research Visits Project supported by Disaster Prevention Research Institute of Kyoto University (Grant No. 27S-02), and the Fundamental Research Funds for the Central Universities of Hohai University (Grant No. 2016B05214).

*Corresponding author. E-mail: jhzheng@hhu.edu.cn

ergy density is smaller than that in deep water areas.

Unlike the previous mechanical and electrical orientations, this research focuses on enhancing the wavy energy density in coastal regions by amplifying its free surface fluctuations based on one classical type of the wave-bottom resonant interaction - Bragg resonance. This resonance, firstly proposed in X-ray crystal reflection in 1910s, when the spacing of the crystal is an integer multiple of the half wave length of the incident wave, the reflection of X-ray through two parallel crystals is the strongest. Then it was introduced to the water wave theory from 1980s with plenty of studies afterwards. Similarly, when the water waves propagate through the periodic topography (rippled bottoms) and the rippled bottoms' wave length is an integer multiple of the half wave length of the incident waves (especially when the free surface wavelength is twice the bottom wavelength), the Bragg resonance will also occur. Then strong reflected waves are induced (large amount of the wave energy is reflected) and intensive oscillations (partial standing waves) are generated on the seaward free surface above the wavy bottoms.

From the preliminary investigations of Davies (1982a, 1982b), Heathershaw (1982) and Davies and Heathershaw (1984), this special phenomenon for water waves began to acquire a lot of concerns. Based on the previous experiment and linear solutions, more analysis methods were utilized by Mei (1985), Kirby (1986, 1988), Dalrymple and Kirby (1986), and Davies et al. (1989). Then more types of the Bragg resonance were introduced by Belzons et al. (1991), Guazzelli et al. (1992) and Liu and Yue (1998). This interaction usually exists in the nearshore area and involves continuous submarine periodic wavy bottoms which are either naturally existing serial undersea sandbars or multiple artificial submerged long-crest structures. For naturally existing sandbars, they were found at many estuaries and coastal regions in China, such as the Yangtze River Estuary and the Pearl River Estuary (Yang et al., 1999; Sun et al., 2010). For artificial submerged structures, the coastal defense engineering based on Bragg resonance induced by multiple series artificial submerged breakwaters was studied. Hsu et al. (2002) compared various shapes of the multiple artificial submerged breakwaters by numerical study based on the expanded elliptic mild slope equation. Cai (2003) found that the Bragg reflection bandwidth will increase for a series of submerged breakwaters on the slope bottom by experiment. Wen and Tsai (2008) studied the parameter effects on the reflection bandwidth and maximum reflection coefficient based on the expanded elliptic mild slope equation and the collected previous researches.

Once the Bragg resonance is triggered, the maximum wave height of the partial standing waves on their antinodes will be larger than that of the original incident waves. Owing to its wave energy concentration in the form of partial standing waves by reflecting the incident wave power, this resonant interaction becomes an alternative to increase the wave amplitude and enhance the wave energy density and wave power capture at specific nearshore regions.

So, a series of flume experiments were performed to study the enhancement of the wave energy extraction by Bragg resonance quantitatively. The model of a point absorber was settled in the wave flume to convert the wave energy into mechanical energy. And a permanent magnet single phase linear motor was utilized to generate electricity. The effects of different incident wave periods and water depths on wave energy extraction were analyzed to find out the features of the wave-power enhancement by Bragg resonance. This study combines the Bragg resonance in water wave hydrodynamics and the practical application of wave energy power generation.

## 2 Experimental setup and process

Based on a wave flume and a point wave energy absorber, the experiment was performed in the Estuary Waterway Experiment Hall of Hohai University. The total length of the wave flume is 67 m. And the height and width are 1.5 m and 1.0 m, respectively. The incident regular waves were generated by the paddle wave maker. At the end of the wave flume, the rubble slope was settled to dissipate the incident waves (Fig. 1).

Five fixed continuous sinusoidal wavy bottoms were installed to induce the Bragg resonance. The wavy bottoms' wave length is 0.9 m and the height is 0.3 m. So the steepness (the ratio of the bottom wave height to the bottom wave length) of the bottom undulation is 0.3 which is large enough to trigger intensive Bragg resonance and reflect a large amount of the incident wave energy (Fig. 2). These sinusoidal wavy bottoms were installed with a distance of 36.75 m to the wave maker. And the distance between these

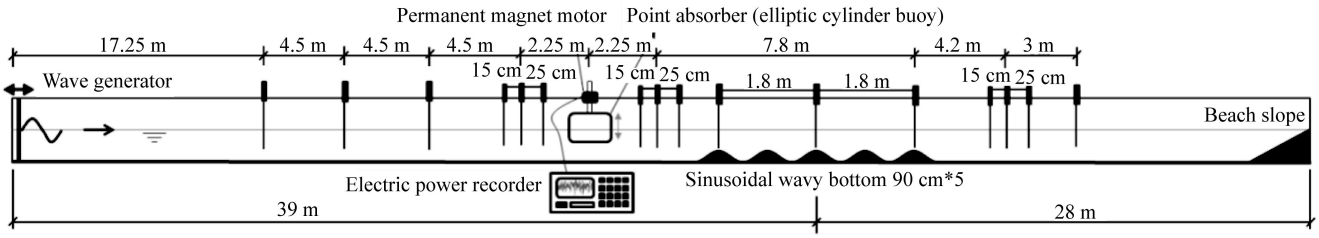


**Fig. 1.** Experimental set-up of the wave-power enhancement by Bragg resonance.

**Fig. 2.** Continuous sinusoidal periodic topography on the bottom of the flume.

**Fig. 3.** A point absorber made by hollow steel oscillating buoy of elliptic cylinder.

bottoms and the slope of the end is 25.75 m. It has enough space for the reflected wave to propagate from the wavy bottoms to the wave maker, also for the transmitted wave to propagate from the bottoms to the end slope. So it ensures enough time for wave gauges to record the free surface signal without the effects of the reflection from the wave maker and rubble slope.

Sixteen capacitive wave gauges were installed along the wave flume. Among them, three groups of the wave gauges were set to separate the incident and reflected wave signals. They were installed on the upstream side of the point absorber, between the point absorber and the wavy bottoms, and on the downstream side of the bottoms respectively in order to measure the reflection coefficients of the point absorber, wavy bottoms and the endmost rubble slope. In each group, three wave gauges were used for wave separation by Mansard's incident and reflected wave separation method (Mansard and Funke, 1980). Besides, three wave gauges were arranged between the wave maker and the point absorber with a 4.5 m neighboring distance. The other three gauges were set above the sinusoidal wavy bottoms. And one wave gauge was set at the downstream side near the rubble slope.

For wave power extraction, a point absorber was made by a hollow steel buoy of elliptic cylinder, which was installed at the incident side of the wavy bottoms with a distance of 33 m to the wave maker. Its horizontal cross-section's major and minor axes are 0.75 m and 0.3 m, respectively. The reason to choose the absorber with an elliptic horizontal cross-section is to reduce the reflection effect of incident waves by the absorber itself (its minor axis occupies less space of the flume's width) and stabilize the wave field along the flume. Besides, the absorber's height is 0.3 m and the weight is 25 kg. Its top cap was welded to a vertical pipe which moves with the absorber and induces the relative vertical displacement to the stator (Fig. 3). The stator was fixed above the point absorber and it was the main part of a permanent magnet single phase linear motor for wave energy conversion. The performance of this motor has been introduced by Yu et al. (2012) and Huang et al. (2013). The electrical signals outputted from the motor were collected and recorded by the electric power recorder.

In this experiment, in order to generate obvious Bragg resonance and avoid the wave breaking above the topography, the wave depths were chosen of 0.6 m, 0.7 m and 0.8 m. All the incident waves were regular, and the incident wave height was a constant of 0.08 m. According to the dispersion relation, the incident wave period corresponding to the resonance peak was 1.15 s, so the incident wave periods covered the vicinity of the resonance as well as the range outside it. For this experiment, the incident wave period varied from 1.0 s to 1.4 s with the values of 1.0 s, 1.1 s, 1.15 s, 1.2 s, 1.3 s and 1.4 s at each water depth. Therefore, the wave period of the incident wave as well as the water depth varies along with the influence factors, and they altered the intensity of the Bragg resonance and the energy extracted by the wave-power equipment.

It should be noted that, before the experimental case study, we tested the point absorber's response by different incident wave periods in order to determine its inherent resonant period. During the test, the wave height and water depth kept constant. And the collected electric power of the point absorber was recorded. It showed that the designed range of the incident wave period (1.0–1.4 s) was contained in the inherent period range of the point absorber.

During the experiment, the wave energy conversion by the point absorber without the wavy bottom was measured firstly on the flat bottom for comparison. After the absorber was removed and the wavy bottoms were installed, the free surface was measured when the incident waves propagated over the wavy bottoms. So the locations of the antinodes were identified when strong Bragg resonance occurred. Then the wavy bottoms were kept in the flume and the absorber was installed in the flume again at the selected antinode locations. And the wave energy conversion was measured by the electric recorder in order to acquire the effects of Bragg resonance.

## 3 Results and discussions

To illustrate the enhancement of the wave power extrac-

tion by Bragg resonance, the comparisons focus on the electrical characteristics measured by an electric power recorder between the cases with and without Bragg resonance. Firstly, the reflection coefficient of the incident wave by the wavy bottoms (Bragg reflection) will be presented with and without the effect of the point absorber. So, the hydrodynamic features of the Bragg resonance will be shown. And the influence of the point absorber on the wave field in the flume will be evaluated for the experiment's feasibility. Then by focusing on the cases when the intensive Bragg resonance occurs, the time-varied voltage and active power with and without Bragg resonance (wavy bottoms) will be compared. At last, for all the cases stated in this paper, their comparisons of the extracted wave power with and without Bragg resonance will be presented.

### 3.1 Reflection coefficients of the Bragg resonance with and without a point absorber

The free surface responses of the wave reflection by sinusoidal bottoms are stated in this section. The reflection coefficients are calculated by the incident and reflected wave separation method proposed by Mansard and Funke (1980). The calculation is based on three wave gauges' data in one wave gauge group at the incident side of the wavy bottoms.

In each water depth, the variety of the reflection coefficient with different dimensionless wave numbers ($2k/k_b$, $k_b$ is the bottom wave number, and $k$ is the incident free-surface wave number varying with different wave periods) is presented. It shows the distribution of the intensity of Bragg resonance with various incident wave periods. Besides, the reflection coefficients corresponding to the cases with and without the point absorber (the point absorber was not installed) are compared to show the influence of the point absorber on the wave field.

Fig. 4 is the distribution of the reflection coefficient with the variety of dimensionless wave numbers with and without the point absorber when the water depth keeps constant of 0.6 m. It shows that when the incident wave period was around 1.15 s and 1.2 s, the Bragg resonance was intensively triggered and strong wave energy reflection occurred. The reflection coefficient could reach 0.54 as the reflection peak corresponds to the dimensionless wave number of 0.85. But the strong reflection (resonance) just occurred in a narrow range of the incident wave periods. Besides, for the scenarios with the point absorber, the reflection coefficient curve is basically the same with the cases without the point absorber. It shows that the effect of the designed point absorber (with a horizontal elliptic cross-section) on the wave field in the wave flume is small and could be neg lected. And it also ensures the accuracy of this experiment.

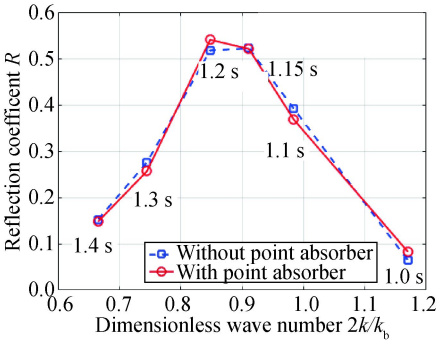


**Fig. 4.** Reflection coefficient of the Bragg resonance by wavy bottoms with and without a point absorber at the water depth of 0.6 m.

The comparison of the Bragg resonance reflection coefficient between the present experiment without the point absorber at the water depth of 0.6 m and perturbation theory (Mei, 1985) is presented in Fig. 5. It should be noted that, due to the average water depth above the wavy bottoms is less than the water depth on the flat bottom in the present experiment, the water depth value substituted in Mei's perturbation theory is the difference between the water depth on the flat bottom and the bottom amplitude. The reflection coefficient value from the experiment is quantitatively consistent with Mei's theory, but the condition of the resonance peak is deviated from the theory due to the frequency downshift which was also found by previous flume experiments. Liu (1994) illustrated some properties of this frequency downshift of Bragg resonance by theoretical calculation. And the detailed properties of the frequency downshift need further theoretical and experimental investigation in the future.

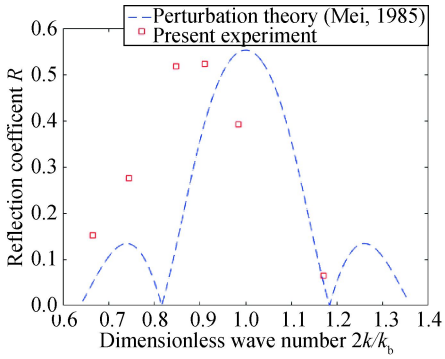


**Fig. 5.** Comparison of the Bragg resonance reflection coefficient between the present experiment without a point absorber at the water depth of 0.6 m and perturbation theory (Mei, 1985).

For the water depths are 0.7 m and 0.8 m, the maximum value of the reflection coefficient decreased with the larger water depth. The intensity of Bragg resonance deteriorates when the distance between the free-surface and wavy bottoms increases. When the water depth is 0.7 m (Fig. 6), the peak value of the reflection coefficient decreases to 0.34 at the dimensionless wave number $2k/k_b$ of 0.89. When the water depth is 0.8 m (Fig. 8), the peak value of the reflection coefficient decreases further to only 0.195 at the dimension-

less wave number $2k/k_b$ of 0.96. The comparisons of the Bragg resonance reflection coefficient between the present experiment without a point absorber at the water depths of 0.7 m and 0.8 m and perturbation theory (Mei, 1985) are presented in Figs. 7 and 9. The values of reflection coefficients are quantitatively consistent with the theory except for the frequency downshift of the peak reflection.

Generally, with the dimensionless wave number ranging from 0.8 to 1.0, the Bragg reflection induced by wavy topography is relatively intensive for enhancing the wave

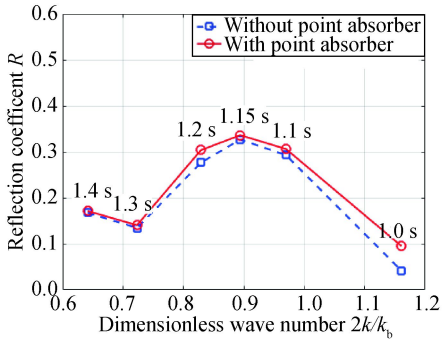


**Fig. 6.** Reflection coefficient of the Bragg resonance by wavy bottoms with and without a point absorber at the water depth of 0.7 m.

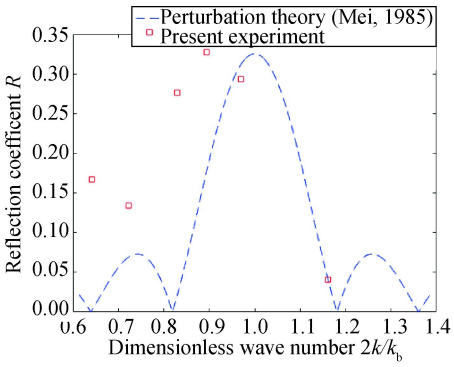


**Fig. 7.** Comparison of the Bragg resonance reflection coefficient between the present experiment without a point absorber at the water depth of 0.7 m and perturbation theory (Mei, 1985).

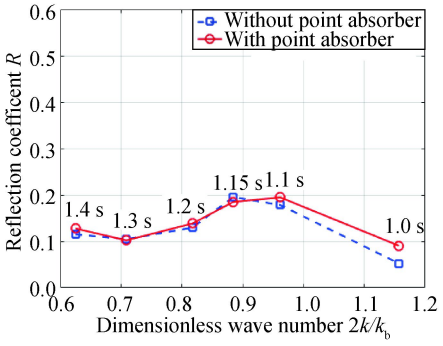


**Fig. 8.** Reflection coefficient of the Bragg resonance by wavy bottoms with and without a point absorber at the water depth of 0.8 m.

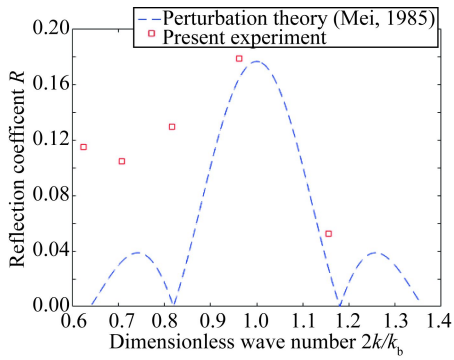


**Fig. 9.** Comparison of the Bragg resonance reflection coefficient between the present experiment without a point absorber at the water depth of 0.8 m and perturbation theory (Mei, 1985).

power capture. So it is the resonant band corresponding to the incident wave periods from 1.1 s to 1.2 s. It should be noted that the dimensionless wave number corresponding to the resonant peak shifts down from the unity when the water depth decreases. So the wave depth not only affects the intensity of Bragg resonance, but also alters the resonant peak. Besides, there is still no obvious difference between the cases with and without the point absorber.

Larger reflection coefficient will induce larger amplitude partial standing waves on their antinodes. Based on Eqs. (1) and (2) for calculation of the partial standing waves, the wave height will be amplified by 54% at the antinode when the reflection coefficient reaches 0.54 at the resonant peak of the water depth of 0.6 m.

$$K_r = \frac{A_r}{A_i} = \frac{A^*_{max} - A^*_{min}}{A^*_{max} + A^*_{min}}; \tag{1}$$

$$\begin{cases} A^*_{max} = A_i + A_r \\ A^*_{min} = A_i - A_r \end{cases} \tag{2}$$

where $A_r$ and $A_i$ are the amplitudes of reflected and incident waves, respectively; $K_r$ is the reflection coefficient. But at the node of the partial standing waves, the wave height will be deteriorated to only 46% of the incident wave height. Therefore, in order to guarantee the wave power enhancement, the point absorber must be installed in the location near or at the antinode.

### 3.2 Comparison of the measured voltage with and without Bragg resonance

According to the experiment cases before, the locations of node and antinode were measured when partial standing waves were generated by Bragg resonance. Then a point absorber was installed in the flume at the antinode for the wave power enhancement.

The case with the most intensive Bragg reflection ($T$=1.15 s, $h$=0.6 m) is chosen to show the enhancement of the wave power (Fig. 10). The time-varied instantaneous voltage was measured at the output side of the permanent magnet single phase linear motor. The sampling time and

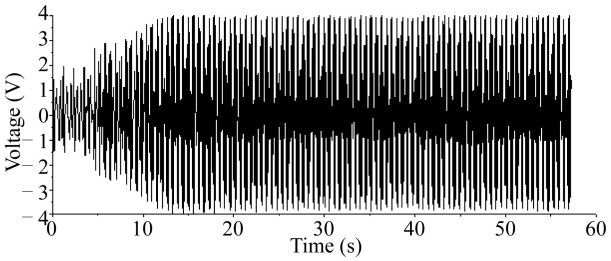


**Fig. 10.** Time series of the voltage extracted by a linear generator before and after the Bragg resonance occurs ($T$=1.15 s, $h$=0.6 m).

frequency were 60 s and 1000 Hz. And the sampling began when the incident wave started to propagate through the point absorber. It shows that when the intensive Bragg resonance was triggered and the wave energy was reflected by wavy bottoms, the output voltage generated by the point absorber and its motor can be dramatically improved and kept stable at the high value of the voltage (about 4 V in amplitude).

For comparison, the time series of the instantaneous voltage measured at the same incident wave elements' condition in the flat flume (without the wavy bottoms and Bragg resonance) are presented (Fig. 11). It shows a huge difference between the voltage extracted by the point absorber under the same condition of the incident waves with and without Bragg resonance. Without Bragg resonance, although the instantaneous voltage rises suddenly at the initial stage due to the point absorber encounters the wave front, the voltage keeps stable to lower value after 30s at about 1.5V in amplitude. It should be noted that the difference of the voltage time series in Fig. 8 before and after 35s is mainly due to the beach reflection at the endmost rubble slope in the flume.

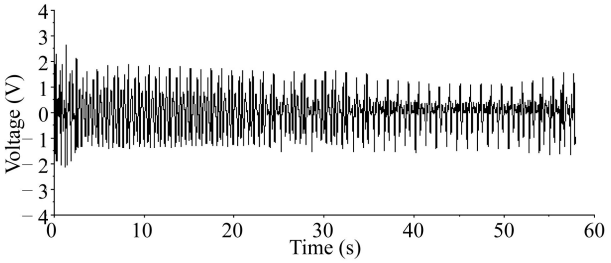


**Fig. 11.** Time series of the voltage extracted by a linear generator on the flume of a flat bottom (with the same incident wave in Fig. 7).

### 3.3 Characteristics of the wave power enhancement (comparison of the active power)

For further quantitative comparison, the active power is calculated to show the extracted wave energy. The active power is the power in the load at the electric circuit. It is calculated based on the Fourier transmission of the time series of the fundamental waves' voltage and current by real-time measurement. Then the amplitude and the phase of the fundamental waves' voltage and current will be acquired. And the active power is calculated by the following equation.

$$P = UI\cos(\varphi_U - \varphi_I), \tag{3}$$

where $P$ is the active power, $U$ is the voltage, $I$ is the current, $\varphi_U$ is the phase of the voltage, and $\varphi_I$ is the phase of the current.

For the average active power $\bar{P}$, the average of the instantaneous power integration in the load at the electric circuit is calculated. In each case, the stable part of the instantaneous active power is selected to calculate the average value of the active power. And the duration involved in the calculation keeps same at different cases. The formula of the average value of active power is

$$\bar{P} = \frac{1}{n}\sum_{i=1}^{n} P(t_i). \tag{4}$$

By calculating the average active power, the comparisons of the converted electric energy with and without Bragg resonance are presented. The cases without Bragg resonance were made in the flume with flat bottoms (no wavy bottoms were installed).

When the water depth is 0.6 m, the most obvious difference of the active power is shown in Fig. 12. For the cases without sinusoidal topography, the active power decreases slightly when the dimensionless wave number increases, and its maximum average power value is reached at $T$=1.4 s of the value of 0.0055 W. For the cases with Bragg resonance, the peak value of active power is 0.034 W at $T$=1.15 s and it is much larger than that without resonance. The distribution curve of the active power is similar to the pattern of the reflection coefficient. This results show that the active power captured by point absorber raises dramatically when the intensive partial standing waves are generated by Bragg resonance (up to 0.034 W). In the presence of the wavy bottoms, the captured active power enhances about 11.5 times comparatively under the most intensive resonant condition (the active power captured at $T$=1.15 s and $h$=0.6 m under the resonance is 12.5 times the active power without resonance under the same wave condition). It shows that it is

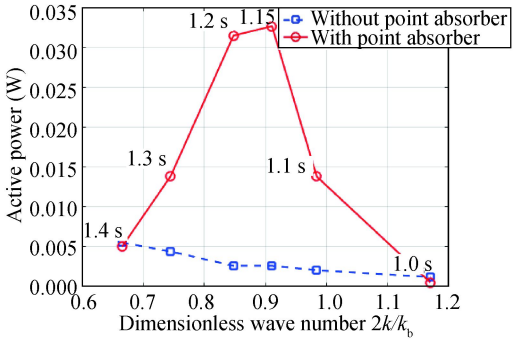


**Fig. 12.** Comparison of the active power extracted with and without Bragg resonance ($h$=0.6 m).

feasible to enhance the wave power extraction by Bragg resonance in nearshore regions.

Although the wave height at antinode reaches 1.54 times the incident wave height when the reflection coefficient induced by Bragg resonance is 0.54 at $T$=1.15 s and $h$=0.6 m, the amplification of the wave power enhancement captured by the point absorber at antinode (12.5 times) is much larger than the amplification of the wave height (1.54 times). The contribution to this phenomenon may be twofold or more. The first reason is that, with the increment of the antinodes' oscillating amplitude induced by Bragg resonance, wave energy is proportional to the square of the wave height. Besides, the motion characteristics of the free surface water particle are another key point to the wave power enhancement for the point absorber. There are obvious differences of kinetic features between propagating waves and standing waves. For the same wave height of the propagating waves and the standing waves at antinode, the behaviors of the oscillating motion of the point absorber differ a lot. The corresponding velocity and acceleration show the different patterns. The water particles move vertically at antinodes of standing waves. So it will be more efficient for the point absorber to convert and generate energy under the condition of standing waves or partial standing waves. It is not only feasible, but also an effective way to improve the wave energy extraction by Bragg resonance with the point absorber in the nearshore areas with continuous sandbars or multiple submerged breakwaters.

It should be noted that, when the Bragg resonance is pretty weak (corresponding to the incident wave period smaller than 1.0 s and larger than 1.4 s), the wave power generation with and without resonance has no obvious difference. The active power curves intersect at both sides. So the enhancement of the wave energy extraction just limits in a certain region of the resonant band.

Then the comparisons of the active power extracted with and without Bragg resonance for water depths of 0.7 m and 0.8 m are presented (Figs. 13 and 14). When the water depth is 0.7 m, the peak value of the average active power at resonance decreases to 0.015 W. And when the water depth is

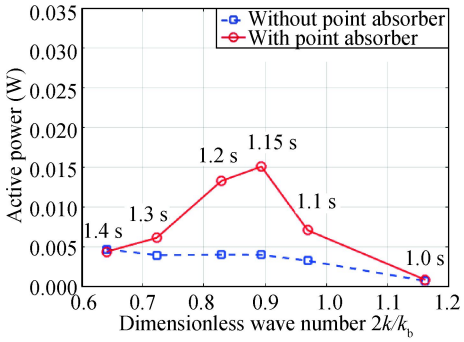


**Fig. 13.** Comparison of the active power extracted with and without Bragg resonance ($h$=0.7 m).

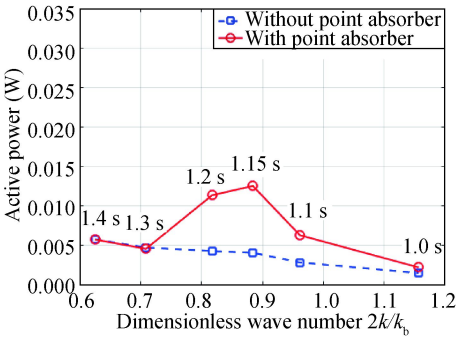


**Fig. 14.** Comparison of the active power extracted with and without Bragg resonance ($h$=0.8 m).

0.8 m, the peak value of the average active power at resonance declines further to 0.0125 W. The increasing water depths weaken the intensity of Bragg resonance, so the enhancement of the active power attenuates similarly. Although the attenuation occurs at larger water depth, it still has good performance on wave power enhancement. For the depth of 0.7 m, the wave power generation efficiency is enhanced 2.73 times by resonance when the incident wave period is 1.15 s. For the depth of 0.8 m, the wave power generation efficiency is enhanced of 2.07 times by resonance when the incident wave period is 1.15 s.

## 4 Conclusion

This experiment shows a robust way to improve the efficiency of the wave power extraction based on a classical wave hydrodynamic phenomenon, the Bragg resonance. The reflection coefficients measured by wave gauges reflect the features of Bragg resonance. And the electricity extracted by an electric power recorder shows the quantitative enhancement of the wave energy collection. It reveals that strong wave reflection induced by Bragg resonance is effective to amplify the free surface oscillation amplitude at the antinodes and focus the wave energy in these regions. More importantly, the electricity generated by the point absorber along with the permanent magnet single phase linear motor shows a remarkable increase of the energy extraction from a standing wave field compared with that from a propagating wave field. When the point absorber moves at the antinodes, it takes the advantage of the kinematic characteristics of water particle on partial standing waves. However, this resonance just occurs in the vicinity of the resonant peak and the wave height enhancement just focuses on the antinode area, so the techniques to enlarge the resonant range and maintain the point absorber's location at antinode is important to improve its applicability for the future study.

## References

Belzons, M., Rey, V. and Guazzelli, E., 1991. Subharmonic Bragg resonance for surface water waves, *EPL* (*Europhysics Letters*), 16(2),

189.

Cai, L.H., 2003. *Bragg Reflection of Water Waves by A Series of Submerged Breakwaters*, Ph.D. Thesis, National Cheng Kung University. (in Chinese)

Dalrymple, R.A. and Kirby, J.T., 1986. Water waves over ripples, *Journal of Waterway*, *Port*, *Coastal*, *and Ocean Engineering*, 112 (2), 309–319.

Davies, A.D., 1982a. On the interaction between surfacewaves and undulations on the seabed, *Journal of Marine Research*, 40(2), 331–368.

Davies, A.G., 1982b. The reflection of wave energy by undulations on the seabed, *Dynamics of Atmospheres and Oceans*, 6(4), 207–232.

Davies, A.G. and Heathershaw, A.D., 1984. Surface-wave propagation over sinusoidally varying topography, *Journal of Fluid Mechanics*, 114, 419–443.

Davies, A.G., Guazzelli, E. and Belzons, M., 1989. The propagation of long waves over an undulating bed, *Physics of Fluids A*: *Fluid Dynamics*, 1(8), 1331–1340.

Falcão, A.F.D.O., 2010. Wave energy utilization: A review of the technologies, *Renewable and Sustainable Energy Reviews*, 14(3), 899–918.

Guazzelli, E., Rey, V. and Belzons, M., 1992. Higher-order Bragg reflection of gravity surface waves by periodic beds, *Journal of Fluid Mechanics*, 245, 301–317.

Heathershaw, A.D., 1982. Seabed-wave resonance and sand bar growth, *Nature*, 296(5855), 343–345.

Hsu, T.W., Chang, H.K. and Tsai, L.H., 2002. Bragg reflection of waves by different shapes of artificial bars, *China Ocean Engineering*, 16(3), 343–358.

Huang, L., Yu, H.T., Hu, M.Q., Liu, C.Y.and Yuan, B., 2013. Research on a tubular primary permanent-magnet linear generator for wave energy conversions, *IEEE Transactions on Magnetics*, 49(5), 1917–1920.

Kirby, J.T., 1986. A general wave equation for waves over rippled beds, *Journal of Fluid Mechanics*, 162, 171–186.

Kirby, J.T., 1988. Current effects on resonant reflection of surface water waves by sand bars, *Journal of Fluid Mechanics*, 186, 501–520.

Liu, Y.M., 1994. *Nonlinear Wave Interactions with Submerged Obstacles with or Without Current*, Ph.D. Thesis, Massachusetts Institute of Technology, Massachusetts.

Liu, Y.M. and Yue, D.K.P., 1998. On generalized Bragg scattering of surface waves by bottom ripples, *Journal of Fluid Mechanics*, 356, 297–326.

Mansard, E.P.D. and Funke, E.R., 1980. The measurement of incident and reflected spectra using a least squares method, *Proceedings of the 17th International Conference on Coastal Engineering*, Sydney, Australia, 154–163.

Mei, C.C., 1985. Resonant reflection of surface water waves by periodic sandbars, *Journal of Fluid Mechanics*, 152, 315–335.

Shi, W.Y., Wang, C.K. and Shen, J.F., 2011. Utilization and prospect of ocean energy resource in China, *Acta Energiae Solaris Sinica*, 32(6), 913–923. (in Chinese)

Sun, J., Zhan, W.H., Jia, J.Y. and Qiu, X.L., 2010. Hazardous geology and its relationship with environmental evolution in the Pearl River Estuary, *Journal of Tropical Oceanography*, 29(1), 104–110. (in Chinese)

Wen, C.C. and Tsai, L.H., 2008. Numerical simulation of Bragg reflection based on linear waves propagation over a series of rectangular seabed, *China Ocean Engineering*, 22(1), 71–86.

Yang, S.L., Zhang, Z.T., Xie, W.H. and He, S.L., 1999. A study of sand waves in the South Channel of the Yangtze Estuary, *The Ocean Engineering*, 17(2), 88–94. (in Chinese)

Yu, H.T., Liu, C.Y., Yuan, B., Hu, M.Q., Huang, L. and Zhou, S.G., 2012. A permanent magnet tubular linear generator for wave energy conversion, *Journal of Applied Physics*, 111(7), 07A741.

Zhang, J., Yu, H.T., Chen, Q. and Hu, M.Q., 2013. Dynamic characteristics and experiment analysis of a single phase permanent magnet linear generator for wave energy conversion, *Transactions of China Electrotechnical Society*, 28(7), 110–116. (in Chinese)